Dalton Transactions

Synthesis, structures and luminescent properties of amine-bis(N-heterocyclic carbene) copper(I) and silver(I) complexes

Journal:	*Dalton Transactions*
Manuscript ID	DT-ART-02-2018-000599.R1
Article Type:	Paper
Date Submitted by the Author:	10-Apr-2018

Complete List of Authors:	Lu, Taotao; Coordination Chemistry Institute, State Key Laboratory of Coordination Chemistry Wang, Jin-Yun; Fujian Institute of Research on the Structure of Matter, State Key Laboratory of Structural Chemistry Shi, Lin-Xi; Fujian Institute of Research on the Structure of Matter, CAS, State Key Laboratory of Structural Chemistry Chen, Zhong-Ning; Fujian Institute of Research on the Structure of Matter, CAS, State Key Laboratory of Structural Chemistry Chen, Xue-tai; Coordination Chemistry Institute, State Key Laboratory of Coordination Chemistry; Xue, Ziling; University of Tennessee, Department of Chemistry

SCHOLARONE™
Manuscripts

Synthesis, structures and luminescent properties of amine-bis(N-heterocyclic carbene) copper(I) and silver(I) complexes

Taotao Lu,[a,#] *Jin-Yun Wang,*[b,#] *Lin-Xi Shi,*[b] *Zhong-Ning Chen,*[b,*] *Xue-Tai Chen,*[a,*] *Zi-Ling Xue*[c]

.

Abstract

A series of Ag(I) and Cu(I) complexes $[Ag_3(L^1)_2][PF_6]_3$ (**8**), $[Ag_3(L^2)_2][PF_6]_3$ (**9**), $[Cu(L^1)][PF_6]$ (**10**) and $[Cu(L^2)][PF_6]$ (**11**) have been synthesized by reactions of the tridentate amine-bis(N-heterocyclic carbene) ligand precursors $[H_2L^1][PF_6]_2$ (**6**) and $[H_2L^2][PF_6]_2$ (**7**) with Ag_2O and Cu_2O, respectively. Complexes **10** and **11** can also be obtained by transmetalation of **8** and **9**, respectively, with 3.0 equiv of CuCl. A heterometallic Cu/Ag-NHC complex $[Cu_2Ag(L^1)_2(CH_3CN)_2][PF_6]_3$ (**12**) is formed by the reaction of **8** with 2.0 equiv of CuCl. All complexes have been characterized by NMR, electrospray ionization mass spectrometry (ESI-MS), and single-crystal X-ray diffraction studies. The luminescent properties of **10-12** in solution and the solid state have been studied. At room temperature, **10-12** exhibit evident luminescence in solution and the solid state. The emission wavelengths are found to be identical at 483

[a] *State Key Laboratory of Coordination Chemistry, School of Chemistry and Chemical Engineering, Nanjing University, Nanjing 210023, China. E-mail: xtchen@nju.edu.cn.*

[b] *State Key Laboratory of Structural Chemistry, Fujian Institute of Research on the Structure of Matter, Fuzhou 350002, P. R. China. Email: czn@fjirsm.ac.cn.*

[c] *Department of Chemistry, University of Tennessee, Knoxville, Tennessee 37996, USA.*

†Electronic supplementary information (ESI) available: Table for the summary of crystal data and refinement; calculation results.

[#]These two authors contributed equally to this work.

nm in CH_3CN, but they are 484, 480 and 592 nm in the solid state for **10**-**12**, respectively. These results suggest that **12** dissociates into two molecules of **10** and Ag(I) ion in solution. Complex **12** is the first luminescent heterometallic Cu/Ag-NHC complex.

Introduction

In the past years, luminescent Cu(I) complexes have been extensively investigated due to their low cost and considered as possible alternatives to luminescent materials based on heavy-metal complexes.[1] To date the most extensively studied mononuclear luminescent Cu(I) complexes are four-coordinate homoleptic and heteroleptic ones bearing diamine or diphosphine derivatives.[1f,1g,2] The photophysical properties of the four-coordinate Cu(I) complexes have shown to be greatly affected by the flattening distortion in the excited state, resulting in the formation of five-coordinate exciplexes that promotes nonradiative decay.[3] In order to alleviate this disadvantage, one accepted approach is to increase the steric bulk of bidentate ligands to prevent the flattening distortion of the excited state and the non-emissive decay pathway.[1f,1g,2] The second approach is to employ three-coordinate Cu(I) complexes with the assumption that the low coordination number would eliminate the undesired distortion of the excited state.[4,5] Multinuclear Cu(I)-halide clusters have also been extensively studied as the enhanced luminescent Cu(I) complexes due to their increase in structural rigidity and hence high photoluminescence quantum yields.[6]

N-Heterocyclic carbenes (NHCs) can form stable metal complexes because of

their strong σ-donor and air- and moisture-stability, and have often been used as alternatives to phosphines in catalysis.[7] In addition to their applications in catalysis, NHC metal complexes including those of Ir(III) and Pt(II) have been found to exhibit luminescent properties.[8] However, there have been few examples of mononuclear luminescent Cu(I)-NHC complexes with coordination numbers of 2-4.[9-11] Thompson, Gaillard and their coworkers have reported a variety of three-coordinate trigonal Cu(I)−NHC complexes $[(NHC)Cu(N^N)]^{0,+}$ bearing a monodentate NHC ligand and a chelating N^N ligand, which exhibit moderate-to-high emission efficiency.[10]

Metal–metal interactions, such as Pt(II)-Pt(II),[12] Au(I)-Au(I)[13] and Cu(I)-Cu(I)[14] interactions have been found to modify the photophysical properties. To date, binuclear and polynuclear Cu(I)-NHC complexes have also been reported to exhibit photoluminescence, in which the Cu(I)-Cu(I) interactions probably play a key role.[15] The luminescent properties of heterometallic Cu/Au-[16] and Ag/Au-NHC[17] complexes have been relatively unexplored. To our knowledge, there has been only one publication by Braunstein[18] on the heterometallic Cu/Ag-NHC complex but its luminescent property has not been studied.

In this contribution, we present the synthesis, structures and photoluminscent properties of two mononuclear three-coordinate Cu(I)−NHC complexes, $[Cu(L^1)][PF_6]$ (**10**) and $[Cu(L^2)][PF_6]$ (**11**), and a heterometallic Cu/Ag-NHC complex $[Cu_2Ag(L^1)_2(CH_3CN)_2][PF_6]_3$ (**12**) bearing a tridentate amine-bis(N-heterocyclic carbene) ligand. Two Ag(I)-NHC precursors $[Ag_3(L^1)_2][PF_6]_3$ (**8**) and $[Ag_3(L^2)_2][PF_6]_3$ (**9**) are also reported herein. The photophysical studies show that

10-12 show weak to intense photoluminescence in the solid state at room temperature, whereas the emission intensity is nearly indentical in solution.

Results and discussion

Synthesis and characterization of NHC precursors

The NHC precursors $[H_2L^1][PF_6]_2$ (**6**) and $[H_2L^2][PF_6]_2$ (**7**) were prepared via the synthetic procedures shown in Scheme 1. Reaction between N-bis[(benzimidazol-1-yl)ethyl]-4-methylbenzenesulfonamide (**1**)[19] and methyl iodide or benzyl bromide yields the dibenzimidazolium salts **2** or **3**, which was transformed into the derivatives **4** or **5** by removing the Ts group with 48% HBr in the presence of PhOH. Finally, the aqueous solution of **4** or **5** is neutralized with triethylamine and then the counteranion was exchanged with NH_4PF_6 to afford the desired ligand precursors **6** and **7**.

In the NMR spectra of **6** and **7**, the signals of NC*H*N proton appear at 8.80 and 9.80 ppm, and N*C*N carbon atoms at 142.2 and 142.6 ppm, respectively. Electrospray ionization mass spectrometry (ESI-MS) analyses of **6** show the peaks at m/z 167.58, 334.25 and 480.17, which are due to $[M-2PF_6]^{2+}$, $[M-2PF_6-H]^+$ and $[M-PF_6]^+$ species, respectively. Likewise, ESI-MS of **7** exhibits similar patterns with that of **6**.

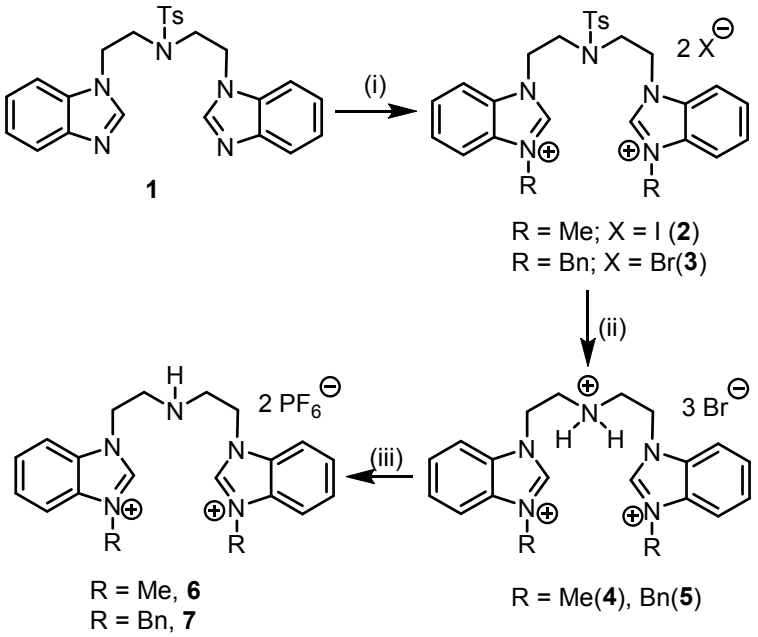

Scheme 1 Synthesis of dibenzimidazolium salts **6** and **7**. Reaction conditions: (i) CH_3I or $PhCH_2Br$, CH_3CN, reflux, 48 h; (ii) PhOH, 48% HBr, 128 °C, 24 h; (iii) Et_3N, H_2O, NH_4PF_6.

Synthesis of metal complexes

Two synthetic routes have been used to prepare Cu-NHC complexes with the tridentate ligands L^1 and L^2. The first approach employed is a carbene transfer reaction using Ag(I)-NHC complex as the precursor, which is a well-established procedure to synthesis metal-NHC including Cu-NHC complexes.[20] Therefore, Ag(I)-NHC complexes derived from the precursors **6** and **7** were firstly synthesized. As shown in Scheme 2, the trinuclear Ag(I)-NHC complexes $[Ag_3(L)_2][PF_6]_3$ (L = L^1, **8**; L = L^2, **9**) were synthesized by reactions of **6** or **7** with 2.0 equiv of Ag_2O in acetonitrile at room temperature for 24 hours. Mononuclear Cu(I)-NHC complexes $[Cu(L)][PF_6]$ (L = L^1, **10**; L = L^2, **11**) were then prepared by carbene transfer reactions

between Ag(I) complexes **8** and **9** with 3.0 equiv of CuCl, respectively. The expected analogous trinuclear Cu(I) complexes were not obtained. Interestingly, it is found that the amount of CuCl is crucial for the identities of the resulting Cu(I) complexes. Reducing the stoichiometry to 2.0 equiv of CuCl per mole of **8** yielded a heterometallic complex $[Cu_2Ag(L^1)_2][PF_6]_3$ (**12**), in which Ag(I) ions have not fully been replaced by Cu(I). Moreover, **12** can further react with CuCl to yield **10** in high yield. Many attempts to prepare similar heterometallic analogue from **9** were unsuccessful, which could be ascribed to the steric bulk of the benzyl substituent. Cu(I) complexes **10** and **11** were also prepared via the second protocol via direct reactions between the respective ligand precursors and excess Cu_2O (Scheme 2).

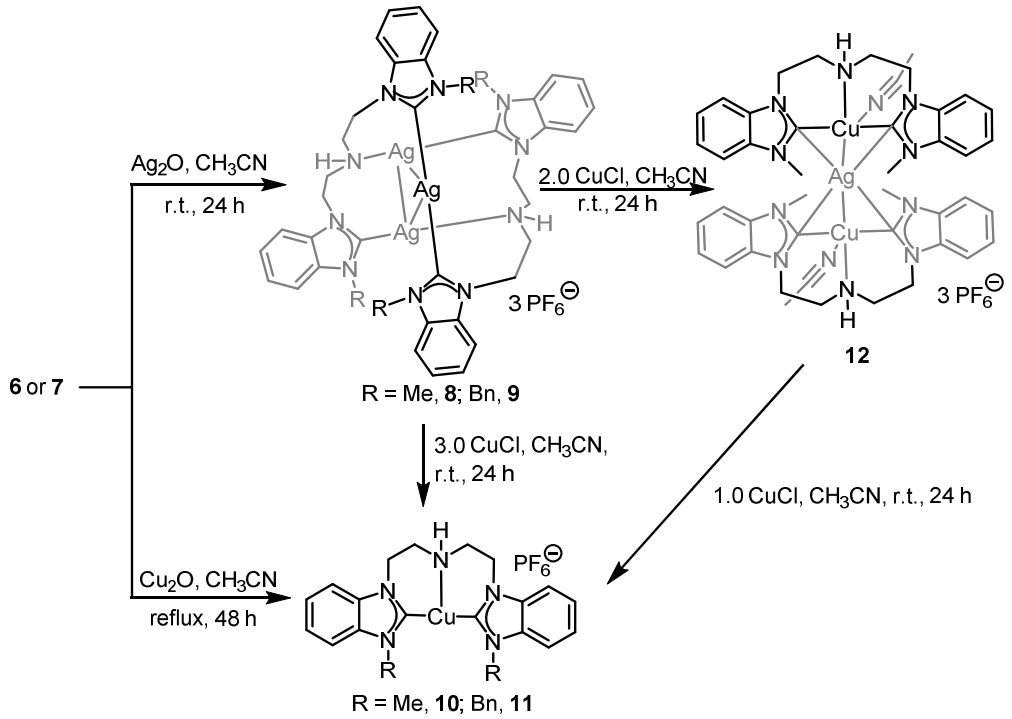

Scheme 2 Synthesis of complexes **8**-**12**.

Complexes **8**-**12** are readily soluble in acetone, acetonitrile, DMF and DMSO,

but insoluble in alcohols and chlorinated hydrocarbons. They are air-stable in the solid state but decompose noticeably in solution. The formation of these complexes has been confirmed by element analysis, NMR spectroscopy, ESI-MS and X-ray crystallography.

The ^{1}H NMR spectra for **8**-**12** show no resonance previously observed for the *2H*-benzimidazolium protons of NHC precursors **6** or **7**, suggesting the coordination of the carbene carbon atom to the metal ion. ^{13}C NMR spectrum shows two resonances at 186.4 and 183.7 ppm for the carbene carbon atoms in **8**, indicating two chemically different carbene carbon atoms. Broad and complicated ^{1}H NMR signals (3.0~8.4 ppm) and several overlapping ^{13}C NMR signals for aromatic rings carbon atoms are found for **9**, which could be due to the fluxionality or the occurrence of several species in solution.[21] This suggests that the Ag_3 core in **9** is not as stable as that in **8** in solution. Complexes **10** and **11** show only one carbene carbon resonance at 188.8 and 190.0 ppm, respectively. ESI-MS peaks at 440.33 and 594.33, corresponding to $[M-Ag-3PF_6]^{2+}$, are found for **8** and **9**, respectively. The peaks corresponding to cation of $[M-PF_6]^{+}$ are detected, respectively, at 396.33 for **10** and 548.33 for **11**. A ESI-MS peak at 396.25 is found for the species $[Cu(L^1)]^{+}$ of **12**. It is worth noting that a ^{1}H NMR signal at 2.06 ppm from free acetonitrile is observed for **12**, indicating that the coordinated acetonitrile ligands dissociate facilely from the Cu(I) centers in solution due to the weak coordination bond Cu-$NCCH_3$. Moreover, the other signals of **12** in both ^{1}H and ^{13}C NMR spectra, as well as ESI-MS signals are identical with those observed for the mononuclear Cu(I) complex **10**, indicating that

12 is dissociated into two molecules of **10** plus Ag(I) ion in solution. This is also consistent with the long distances of Ag-C_{NHC} revealed by X-ray crystallography and the spectral data (see below).

Structural descriptions

Single crystals of **8** were obtained by slow vapor diffusion of ether into an acetonitrile solution of **8**, while crystals of **9**·6CH_3CN were obtained by diffusion of an acetonitrile solution of **9** into toluene. Both complexes crystallize in triclinic space group *P*-1. The structures of the cationic portion of **8** and **9** are shown in Figure 1 with selected structural parameters listed in Table 1.

As shown in Figure 1, complexes **8** and **9** possess similar trinuclear Ag_3 core supported by two amine-bis(NHC) ligands, with Ag−Ag distances of 3.353(2) (Ag1−Ag3), 3.362(2) (Ag1−Ag2) and 3.246(2) Å (Ag2−Ag3) in **8**, and 3.108(2) (Ag1−Ag3), 3.379(2) (Ag1−Ag2) and 3.189(2) Å (Ag2−Ag3) in **9**, respectively. These Ag–Ag distances are within the range reported for similar Ag_3 core NHC complexes.[15e,22] Surprisingly, the Ag1–Ag3 and Ag2–Ag3 distances in **9** are significantly shorter than those in **8**, although **9** contains more sterically encumbering substituent groups (R = Bn) than **8** (R = Me). All Ag−Ag distances are shorter than the sum of van der Waals radii of two Ag ions (3.44 Å), indicating an argentophilic interaction between two Ag(I) centers of each pair in **8** and **9**.[23] In **8**, the Ag1 ion is linearly coordinated to two carbene carbon donors with a C2−Ag1−C33 angle of 175.4(4)°, while Ag2 and Ag3 are coordinated to one carbene carbon and one amine

donors with C13−Ag2−N8 of 165.5(3)° and C22−Ag3−N3 of 167.5(3)°, respectively. Likewise, the Ag ions in **9** adopt similar coordination modes with those in **8**, with C2−Ag1−C33, C13−Ag2−N8 and C22−Ag3−N3 angles of 175.08(18)°, 168.71(15)° and 157.47(16)°, respectively. It is worth noting that the C22−Ag3−N3 bond angle 157.47(16)° in **9** is significantly smaller than that in **8** (167.5(3)°), which could result from the shorter Ag1−Ag3 and Ag2−Ag3 distances in **9**. The Ag−Ag−Ag angles in **8** and **9** are close to 60° (see Table 1). In both complexes, the Ag−C bond distances are found in the range 2.076(10)−2.122(10) Å. The Ag–N bond distances in the range of 2.190(4)−2.200(4) Å are comparable with those in other linear NHC-Ag-amine moiety.[24]

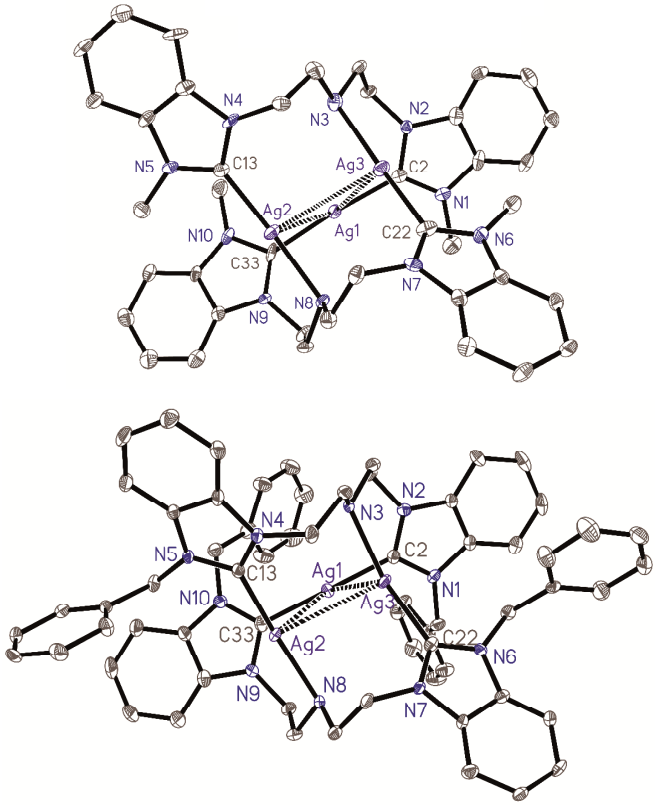

Figure 1 Structures of **8** (top) and **9** (bottom). Anions and hydrogen atoms including

N−*H* are omitted for clarity. Thermal ellipsoids are drawn at 30% probability.

Table 1 Selected bond lengths (Å) and angles (°) of **8** and **9**

	8	**9**
Ag1−C2	2.076(10)	2.081(4)
Ag1−C33	2.103(9)	2.085(5)
Ag2−C13	2.070(9)	2.105(5)
Ag2−N8	2.192(7)	2.200(4)
Ag3−C22	2.122(10)	2.090(4)
Ag3−N3	2.197(8)	2.190(4)
Ag1−Ag3	3.353(2)	3.108(2)
Ag1−Ag2	3.362(2)	3.379(2)
Ag2−Ag3	3.246(2)	3.189(2)
C2−Ag1−C33	175.4(4)	175.08(18)
C13−Ag2−N8	165.5(3)	168.71(15)
C22−Ag3−N3	167.5(3)	157.47(16)
Ag3−Ag1−Ag2	57.82(2)	58.72(2)
Ag3−Ag2−Ag1	60.94(2)	56.38(2)
Ag2−Ag3−Ag1	61.24(2)	64.90(2)

Single crystals of Cu(I) complexes **10**·CH_3CN and **11** suitable for X-ray diffraction analysis were obtained by vapor diffusion of ether into concentrated acetonitrile solutions of complexes **10** and **11**. **10**·CH_3CN crystallizes in monoclinic

space group $P2_1/c$ while **11** in triclinic space group P-1. Their molecular structures are shown in Figure 2, and the selected bond lengths and angles are provided in Table 2. They are mononuclear three-coordinate Cu(I) complexes with *T*-shaped geometry around the center of Cu(I) atom. Similar *T*-shaped configuration has been found in macrocyclic Cu-NHC complex.[25] The Cu−N1 distance of 2.234(2) Å in **10** is very close to 2.202(2) Å in **11**. The Cu−C bond lengths in **10** (1.910(3) and 1.914(3) Å) and **11** (1.920(3) and 1.916(3) Å) fall in the range previously reported for three-coordinate Cu(I)-NHC complexes.[10] The C_{NHC}−Cu−N bond angles in **10** (96.62(10)° and 96.31(9)°) are almost identical to those in **11** (96.24(9)° and 97.74(9)°). The C_{NHC}−Cu−C_{NHC} bond angles are 166.82(11)° and 163.37(11)° for **10** and **11**, respectively. The sum of the bond angles around the copper atom are 359.8° for **10** and 357.4° for **11**, testifying to a slightly distorted planarity.

Table 2 Selected bond lengths (Å) and angles (°) of **10** and **11**

	10	**11**
Cu1−C5	1.910(3)	1.920(3)
Cu1−C13	1.914(3)	1.916(3)
Cu1−N1	2.234(2)	2.202(2)
C13−Cu1−C5	166.82(11)	163.37(11)
C13−Cu1−N1	96.62(10)	96.24(9)
C5−Cu1−N1	96.31(9)	97.74(9)

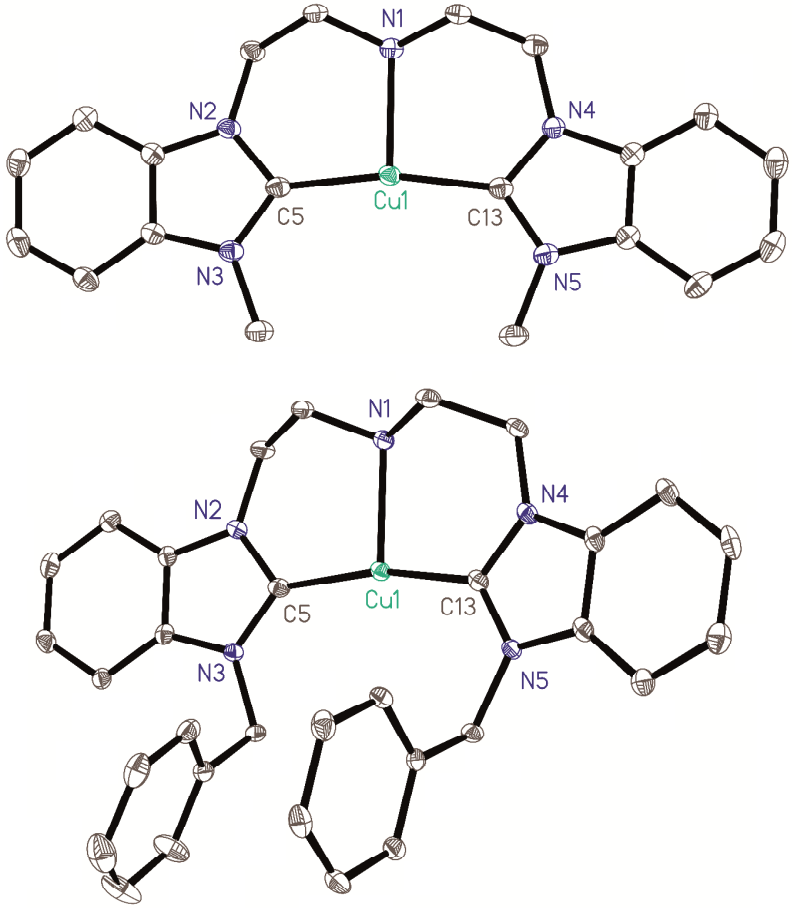

Figure 2 Structures of **10** (top) and **11** (bottom). Anions and hydrogen atoms including N−*H* are omitted for clarity. Thermal ellipsoids are drawn at 30% probability.

Crystals of complex **12** were obtained by vapor diffusion of ether to a solution of **12**. **12** crystallizes as **12**·CH_3CN·0.25H_2O in the monoclinic space group $P2_1/n$. The selected metrical parameters are listed in Table 3. As shown in Figure 3, **12** is a linear trinuclear Cu-Ag-Cu complex with Cu1–Ag1–Cu2 angle of 176.83(14)°, in which Ag1 and Cu1 are bridged by carbene carbon atoms C5 and C13, while Ag1 and

Cu2 are bridged by carbene carbon atoms C27 and C35. Cu1-Ag1 and Cu2-Ag1 distances are 2.477(5) and 2.464(4) Å, respectively, smaller than those in the first mixed Cu/Ag-NHC complex (2.838(1) Å).[18] They are significantly smaller than the sum of van deer Waals radii of copper and silver ions (2.77 Å), suggesting the metallophilic interaction in **12**.[26] Each Cu(I) ion is four-coordinated with the three donors from the tridentate NHC ligand and a nitrogen atom of the acetonitrile molecule. The Cu–C_{NHC} bond lengths in the range from 1.941(3) to 1.958(3) Å are longer than those in **10** and **11** (1.910(3)-1.920(3) Å). However, Cu–N_{amine} bond lengths (2.187(12) and 2.182(2) Å) are similar to those in **10** (2.234(2) Å) and **11** (2.202(2) Å). The Cu–N_{CH3CN} bond lengths are 2.027(2) and 2.079(2) Å. It is interesting to note that the contacts between Ag(I) ion and four carbene carbons between 2.566(3) and 2.797(3) Å are considerably long, suggesting the presence of the weak Ag-NHC interactions. Therefore, the four carbene carbon atoms adopt a semi-bridging mode, which has been only observed in few examples.[27] Complex **12** can be regarded as the coordination of two Cu(I) metalloligands to the central Ag(I) ion via the semi-bridging carbene carbons. The weak Ag-NHC interactions render the dissociation of **12** into two molecules of **10** and an Ag(I) ion in solution, which has been revealed by NMR and ESI-MS data.

Table 3 Selected bond lengths (Å) and angles (°) of **12**

Cu1−C5	1.956(3)	Cu1−C13	1.943(3)	Cu1−N1	2.187(12)
Cu1−N6	2.027(2)	Cu2−C27	1.958(3)	Cu2−C35	1.941(3)
Cu2−N7	2.182(2)	Cu2−N12	2.079(2)	Ag1−C5	2.566(3)
Ag1−C13	2.797(3)	Ag1−C27	2.667(3)	Ag1−C35	2.640(3)
Ag1−Cu1	2.477(5)	Ag1−Cu2	2.464(4)		
C5−Cu1−C13	147.02(12)		C5−Cu1−N1	97.10(13)	
C13−Cu1−N1	95.76(17)		C13−Cu1−N6	105.29(11)	
N6−Cu1−N1	106.9(3)		C5−Cu1−N6	99.77(11)	
C35−Cu2−C27	144.74(12)		C35−Cu2−N7	97.59(10)	
C27−Cu2−N7	97.73(10)		C27−Cu2−N12	101.99(11)	
C35−Cu2−N12	104.50(11)		N12−Cu2−N7	104.74(9)	
C5−Ag1−C27	176.49(8)		C5−Ag1−C35	93.09(9)	
C35−Ag1−C27	88.93(8)		Cu2−Ag1−Cu1	176.83(14)	
Cu1−Ag1−C5	45.60(6)		Cu1−Ag1−C27	132.16(6)	
Cu1−Ag1−C35	138.58(6)		Cu2−Ag1−C5	137.56(6)	
Cu2−Ag1−C35	44.55(6)		Cu2−Ag1−C27	44.67(6)	
C5−Cu1−Ag1	69.59(9)		C13−Cu1−Ag1	77.46(8)	
N1−Cu1−Ag1	115.5(3)		N6−Cu1−Ag1	137.04(7)	
C27−Cu2−Ag1	73.14(8)		N7−Cu2−Ag1	129.10(6)	
C35−Cu2−Ag1	72.53(8)		N12−Cu2−Ag1	126.16(7)	

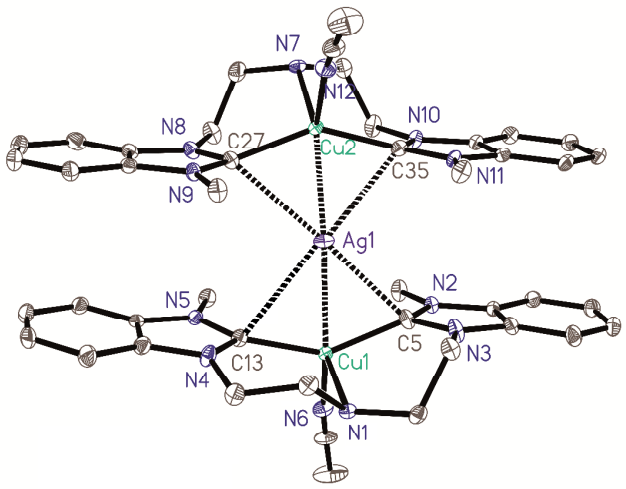

Figure 3 Structure of **12**. Anions and hydrogen atoms including N–*H* are omitted for clarity. Thermal ellipsoids are drawn at 30% probability.

Photophysical properties

The photophysical studies show that the Ag-NHC complexes **8** and **9** are not luminescent in either solution or the solid state while **10-12** are emissive.

The absorption spectra of **10-12** in degassed acetonitrile are presented in Figure 4. The absorption maxima and the corresponding molar extinction coefficients are compiled in Table 4. For **10-12**, the major absorption bands occur between 250 nm and 290 nm with a maximum at 256 nm. Considering the large molar extinction coefficients ($5.94\times10^4 - 7.22\times10^4$ L mol^{-1} cm^{-1}), these absorption bands are ascribed to the ligand-centered (LC) $\pi-\pi^*$ transition. The lower energy bands at ~290−370 nm can be assigned to the $\pi-\pi^*$ transition within the N-heterocycle moiety. The broad and very weak low-energy tails at ~370−430 nm are assigned to the charge transfer

(CT) transitions. It is understandable that similar structured complexes **10** and **11** exhibit nearly the same absorption spectra. But it is interesting that the hetermetallic complex **12** shows the identical absorption spectrum with **10**, which further supports the dissociation of **12** into **10** in solution, in accordance with the NMR, ESI-MS and X-ray structural data.

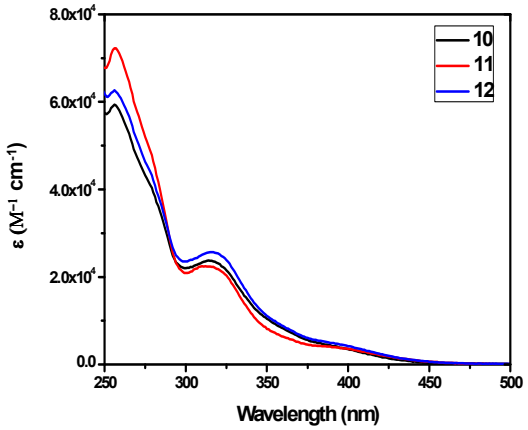

Figure 4 UV−vis absorption spectra of complexes **10-12** in acetonitrile at 298 K (1×10^{-5} M).

Emission spectra of **10-12** recorded at 77 K in frozen 2-methyltetrahydrofuran (2-MeTHF) glass (λ_{ex} = 330 nm) are shown in Figure 5. All three complexes exhibit similar emission properties with a broad structureless band with a large Stokes shift centered at 505 nm for **10**, 499 nm for **11** and 503 nm for **12**, respectively. The emission lifetime of **10-12** are found from 0.75 to 1.03 μs (Table 4). In addition, complexes **10-12** are luminescent in degassed acetonitrile at room temperature, displaying a broad structureless band centered at 483 nm (Figure 5). The quantum yields (Φ_{em}) for **10-12** are found to be 0.18, 0.20 and 0.23, respectively. The excited

state lifetimes are 0.013 μs for **10**, 0.014 μs for **11** and 0.012 μs for **12** (Table 4). The emission wavelength of **10-12** at room temperature exhibits a blue shift of 22 nm for **10**, 16 nm for **11** and 20 nm for **12** relative to 77 K, respectively. Furthermore, shorter emission lifetime was found at room temperature relative to 77 K. The identical luminescent properties of **10** and **12** in acetonitrile and 2-MeTHF suggest that the emissive species are the same three-coordinate copper complex in solution due to the dissociation of **12** into **10**.

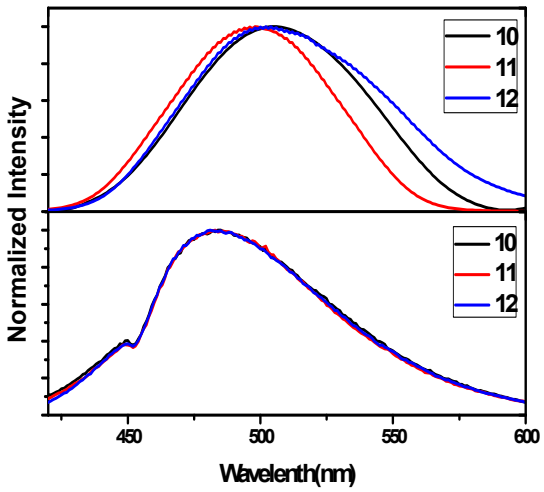

Figure 5 Emission spectra of complexes **10-12** (top, in 2-MeTHF at 77 K; bottom, in acetonitrile at room temperature) in solution (1×10^{-4} M). Excitation wavelength is 330 nm.

Table 4 Photophysical properties of complexes **10**−**12** in solution

		emission at R.T.[a]			emission at 77 K[b]	
Complexes	λ_{max} (nm) (ε, 10^4 M^{-1} cm^{-1})[a]	λ_{em} (nm)	τ (μs)	Φ_{PL}	λ_{em} (nm)	τ (μs)
10	256 (5.94), 314 (2.37), 400 (0.42)	483	0.013	0.18	505	0.75
11	256 (7.22), 312 (2.22), 400 (0.42)	483	0.014	0.20	499	1.03
12	256 (6.24), 316 (2.57), 400 (0.42)	483	0.012	0.23	503	0.78

[a]In acetonitrile. [b]In 2-MeTHF

Photophysical properties for microcrystalline solids of complexes **10**-**12** were also measured at room temperature and 77 K. Emission spectra are shown in Figure 6, and photophysical data are summarized in Table 5. At room temperature, both **10** and **11** exhibit blue emission centered at 484 and 480 nm, respectively. The emission quantum yield of **11** reaches 0.58, which is significantly higher than that of **10** (0.38). The enhancement in emission efficiency of **11** is probably due to the increasing steric bulk of NHC ligands, which could minimize the structural distortion in excited states,[1f,1g,2] and further alleviate the nonradiative decay rate (k_{nr} = 2.2 × 10^4 s^{-1} (**11**) vs 3.7 × 10^4 s^{-1} (**10**)). To our knowledge, the quantum yield found for both **10** and **11** are remarkable for the luminescent Cu(I)-NHC complexes.[9-11] The decay lifetimes of **10** and **11** are 16.7 and 19.1 μs, respectively. These values are characteristic of the triplet

charge transfer state. Upon cooling to 77 K, no obvious spectral change was observed for both **10** and **11**. In addition, the emission lifetime of **10** and **11** measured at 77 K are 24.8 and 26.4 μs, respectively.

Complex **12** exhibits yellow emission centered at 592 nm at room temperature. The significant red shift in the emission spectrum of heterometallic Cu/Ag-NHC complex **12** relative to those of mononuclear Cu(I) complexes **10** and **11** can be ascribed to the metallophilic interactions in **12**.[15d,28] The decay lifetime of **12** is 32.5 μs. The emission quantum yield of **12** was determined to be 0.05, which is significantly smaller than those of both **10** and **11**. These data indicate that the coordination environment about the Cu(I) center have a significant impact on both emission energy and efficiency. Upon cooling to 77 K, **12** undergoes a 20 nm red shift with a much longer lifetime of 86.1 μs.

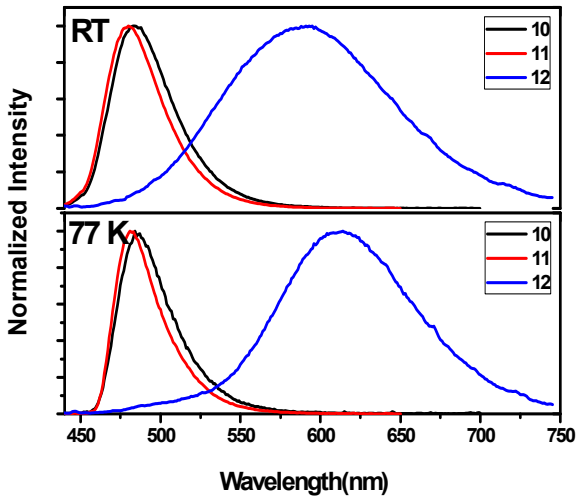

Figure 6 Solid-state emission spectra of complexes **10**−**12** at room temperature (top) and 77 K (bottom). Excitation wavelength is 366 nm.

Table 5 Photophysical properties of complexes **10**–**12** in the solid state

	emission at R. T.					emission at 77 K	
Complexes	λ_{em} (nm)	τ (μs)	Φ_{PL}	k_r (s^{-1})	k_{nr} (s^{-1})	λ_{em} (nm)	τ (μs)
10	484	16.7	0.38	2.3×10^4	3.7×10^4	484	24.8
11	480	19.1	0.58	3.0×10^4	2.2×10^4	481	26.4
12	592	32.5	0.05	1.6×10^3	2.9×10^4	612	86.1

DFT/TD-DFT Computational Studies

TD-DFT computational studies have been performed for complexes **10** and **11** after the DFT geometrical optimization to get insight into the photophysical properties in the CH_3CN solution. The geometrical parameters in the ground state are similar to the experimental crystal data. The optimized structures and the cartesian coordinates of these two complexes in the ground state (S_0) and lowest-energy triplet state (T_1), respectively, are showed in Tables S9-S13. The orbital compositions (%) of different energy levels and the absorption and emission transition characters are detailed in Tables S3-S8. Table 6 summarizes the lowest-energy singlet- and triplet-state transitions of **10** and **11**. The lowest-energy absorption transitions at 399 and 398 nm (S_1) for **10** and **11**, respectively, coincide well with the low-energy absorption in 400 nm showed in Table 4. Likewise, the T_1 transitions located in 514 and 509 nm, respectively, in the CH_3CN solution are also in agreement with the experimental data (487 and 483 nm, respectively, for **10** and **11**). The transitions from the ground state

(S_0) to the singlet (S_1) and triplet (T_1) lowest-energy excited states ($S_0 \rightarrow S_1$ and $S_0 \rightarrow T_1$) of these two complexes mainly involve HOMO→LUMO (no less than 95% contribution). From Tables S3, S5 and S7, and Figure 7, it can be seen that HOMO is mainly populated on the Cu atom (61.09 and 59.26% in the ground state and 59.73 and 59.09 % in the lowest-energy triplet state, respectively, for **10** and **11**) and amine moiety (26.35 and 26.33% in the ground state and 25.65 and 25.57% in the lowest-energy triplet state, respectively, for **10** and **11**), while the LUMO is predominantly contributed by the bis(N-heterocyclic carbene) moiety (80.06 and 80.97% in the ground state and 79.59 and 80.47% in the lowest-energy triplet state, respectively, for **10** and **11**), mixed with some contribution from Cu atom (no more than 15.50%). Therefore, it can be concluded that the low-energy absorption and the emission properties of these two complexes are ascribed to the metal-to-ligand charge transfer (MLCT) transition from Cu atom to bis(N-heterocyclic carbene) moiety, conbined with some ligand-centered (LC) transition from amine to bis(N-heterocyclic carbene) moiety in the amine-bis(N-heterocyclic carbene) ligand.

Table 6 The lowest-energy singlet- and triplet-state transitions for complexes **10** and **11** by TD-DFT method at the PBE1PBE level

Complexes	states	λ (nm)	*f*	Transition (Contri.)
10	S_1	399	0.0132	HOMO→LUMO (96%)
	T_1	514	0.0000	HOMO→LUMO (95%)
11	S_1	398	0.0134	HOMO→LUMO (96%)
	T_1	509	0.0000	HOMO→LUMO (95%)

10	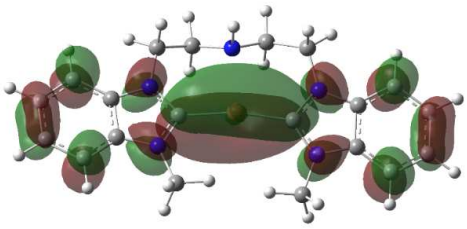	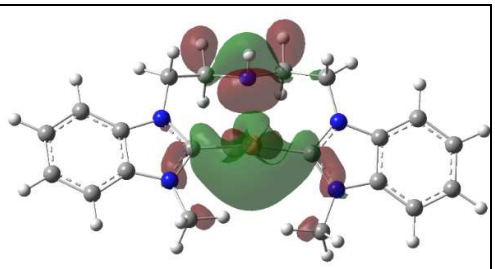
	LUMO	HOMO
11	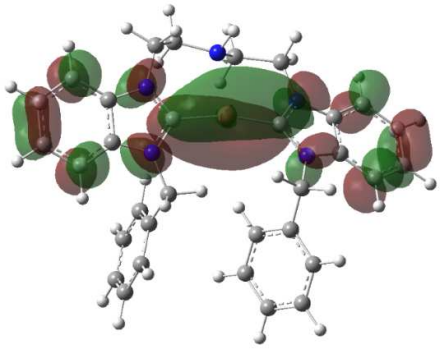	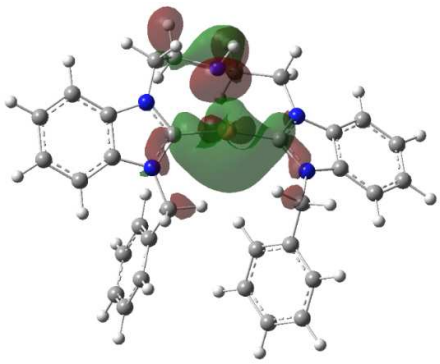
	LUMO	HOMO

Figure 7 Plots of the HOMO and LUMO in the ground state for complexes **10** and **11** in CH_3CN solution by TD-DFT method at the PBE1PBE level (isovalue = 0.025).

Conclusions

In this conbribution, we have presented the synthesis and structural features of two triangular Ag_3 complexes $[Ag_3(L)_2](PF_6)_3$ (L = L^1, **8**; L = L^2, **9**), two three-coordinate Cu(I) complexes $[Cu(L)](PF_6)$ (L = L^1, **10**; L = L^2, **11**) and a heterometallic Cu/Ag complex $[Cu_2Ag(L^1)_2(CH_3CN)_2](PF_6)_3$ (**12**), which bear tridentate amine-bis(N-heterocyclic carbene) ligands. **8** and **9** are new members of the growing family of NHC-bridged triangular structural motifs, which are used as effective transmetalating reagents to prepare the Cu(I) complexes **10**, **11** and heterometallic complex **12**. The photophysical properties of **10-12** have been studied both in solution and the solid state. At room temperature, **10** and **11** have a considerably emission quantum efficiency (0.38 and 0.58, respectively) in the solid state with emission centered at 484 and 480 nm, respectively. However, emission maximum of **12** is significantly red shifted to 592 nm but emission quantum efficiency decrease to 0.05 relative to those of **10** and **11**, indicating that the photophysical properties are dependent on the environment around the metal center. The NMR, ESI-MS and photophysical data reveal that **12** dissociate into two molecules of **10** and Ag(I) ion due to the weak semi-bridging NHC coordination mode.

Experimental section

General procedures

All manipulations were performed under dry nitrogen, using standard Schlenk techniques unless otherwise stated. Acetonitrile was dried over CaH_2 and distilled

under nitrogen before use. All other solvents and chemicals are commercial available and used as received without further purification. The starting material N-bis[(benzimidazol-1-yl)ethyl]-4-methylbenzenesulfonamide (**1**) (Scheme 1) was prepared according to the literature procedures.[19] NMR spectra were recorded on Bruker Avance 400 MHz (^{1}H, 400 MHz; ^{13}C, 100 MHz) spectrometer at 298 K. Elemental analyses (C, H and N) were carried out on a Perkin-Elmer 240C analytic instrument. Mass spectra were measured with ESI-MS (LCQ Fleet, Thermo Fisher Scientific). Electronic absorption spectra were recorded with Shimadzu UV-2550 spectrophotometers. The emission spectra and the emission lifetimes in degassed and oxygen-free solutions were measured in a Model EPL-375 fluorescence spectrometer (Edinburgh Instruments. Ltd, picosecond pulsed diode laser, wavelength 378.2 nm, pulse wildth 78.4 ps). The emission spectra and the emission lifetimes in the solid state were determined on an Edinburgh FLS920 fluorescence spectrometer. The absolute luminescent quantum yields (Φ_{em}) in solid state were determined by the integrating sphere (142 mm in diameter) using an Edinburgh FLS920.

Synthesis of 2 and 3. Methyl iodide or benzyl bromide (87 mmol) in acetonitrile (20 mL) was added dropwise to a stirred solution of **1** (5.0 g, 11 mmol) in acetonitrile (60 mL). The mixture was stirred and refluxed for 48 h. After the solution was cooled down to room temperature, ethyl acetate (100 mL) was added to precipitate a solid, which was filtered and washed with ethyl acetate to afford **2** or **3** as a white solid.

2: 7.3 g (91 % yield). ^{1}H NMR (DMSO-d$_6$, 400 MHz): δ 9.68 (s, 2H, NC*H*N),

7.94−8.15 (m, 4H, bzim), 7.65−7.85 (m, 4H, bzim), 7.30 (d, *J* = 8 Hz, 2H, Ts), 7.08 (d, *J* = 8 Hz, 2H, Ts), 4.77 (br, 4H, bzimCH_2CH$_2$), 4.08 (s, 6H, bzimCH_3), 3.88 (br, 4H, bzimCH$_2$CH_2), 2.27 (s, 3H, PhCH_3). ^{13}C NMR (DMSO-d$_6$, 100 MHz): δ 143.7 (N*C*HN), 142.9, 134.8, 131.6, 130.9, 129.4, 126.6, 126.5, 126.3, 113.6, 113.3, 45.8 (bzimCH$_2$*C*H$_2$NTs), 44.5 (bzim*C*H$_2$CH$_2$NTs), 33.3 (bzim*C*H$_3$), 21.0 (Ph*C*H$_3$). Anal. Calcd for $C_{27}H_{31}N_5I_2SO_2$: C 43.62; H 4.20; N 9.42 %. Found: C 43.45; H 4.31; N 9.27 %.

3: 8.2 g (94 % yield). ^{1}H NMR (DMSO-d$_6$, 400 MHz): δ 10.17 (s, 2H, NC*H*N), 8.06−8.15 (m, 2H, bzim), 7.90−7.98 (m, 2H, bzim), 7.61−7.73 (m, 4H, bzim), 7.55 (d, *J* = 4 Hz, 4H, Ph), 7.32−7.45 (m, 8H, Ts and Ph), 7.09 (d, *J* = 8 Hz, 2H, Ts), 5.83 (s, 4H, PhCH_2), 4.88 (t, *J* = 6 Hz, 4H, bzimCH_2CH$_2$), 3.96 (t, *J* = 6 Hz, 4H, bzimCH$_2$CH_2), 2.28 (s, 3H, CH_3). ^{13}C NMR (DMSO-d$_6$, 100 MHz): δ 143.8 (N*C*HN), 142.7, 134.7, 133.9, 131.3, 130.7, 129.6, 128.9, 128.7, 128.3, 126.8, 126.7, 126.5, 113.9, 113.7, 49.8 (Ph*C*H$_2$), 46.2 (bzimCH$_2$*C*H$_2$NTs), 44.9 (bzim*C*H$_2$CH$_2$NTs), 21.0 (*C*H$_3$). Calcd for $C_{39}H_{39}N_5Br_2SO_2$: C 58.43; H 4.90; N 8.74 %. Found: C 58.21; H 4.79; N 8.66 %.

Synthesis of 4 and 5: **2** or **3** (10 mmol), PhOH (2.8 g, 29 mmol) and 48 % HBr (80 mL) were added to a flask. The mixture was stirred at 128 ^{o}C for 24 h. The mixture was cooled to room temperature, concentrated to about 20 mL and treated with acetone (200 mL) to precipitate a solid, which was filtered and washed with acetone to afford **4** or **5** as a white solid.

4: 5.0 g (88 % yield). ^{1}H NMR (D$_2$O, 400 MHz): δ 9.41 (s, 2H, NC*H*N),

7.85−8.02 (m, 4H, bzim), 7.71−7.82 (m, 4H, bzim), 4.97 (t, *J* = 6.4 Hz, 4H, bzimC*H*$_2$CH$_2$N), 4.14 (s, 6H, bzimC*H*$_3$), 3.83 (t, *J* = 6.4 Hz, 4H, bzimCH$_2$C*H*$_2$N). ^{13}C NMR (D$_2$O-d$_2$, 100 MHz): δ 142.1 (N*C*N), 132.2 (bzim), 130.8 (bzim), 127.5 (bzim), 127.4 (bzim), 113.5 (bzim), 112.6 (bzim), 46.4 (bzimCH$_2$*C*H$_2$N), 47.0 (bzim*C*H$_2$CH$_2$N), 33.3 (bzim*C*H$_3$). Anal. Calcd for C$_{20}$H$_{26}$N$_5$Br$_3$: C 41.69; H 4.55; N 12.16 %. Found: C 41.55; H 4.39; N 11.92 %.

5: 5.4 g (76 % yield). ^{1}H NMR (DMSO-d$_6$, 400 MHz): δ 10.13 (s, 2H, NC*H*N), 9.56 (br, 2H, N*H*$_2$), 8.22 (d, *J* = 8 Hz, 2H, Ph), 7.96 (d, *J* = 8 Hz, 2H, Ph), 7.64−7.78 (m, 4H, bzim), 7.55−7.62 (m, 4H, bzim), 7.34−7.48 (m, 6H, Ph), 5.82 (s, 4H, PhC*H*$_2$), 4.99 (t, *J* = 6 Hz, 4H, bzimC*H*$_2$CH$_2$N), 3.77 (br, 4H, bzimCH$_2$C*H*$_2$N). ^{13}C NMR (DMSO-d$_6$, 100 MHz): δ 143.5 (N*C*N), 133.6, 131.3, 131.0, 128.9, 128.8, 128.5, 126.8, 126.8, 114.0 (114.0), 50.1 (Ph*C*H$_2$), 45.2 (bzimCH$_2$*C*H$_2$N), 43.0 (bzim*C*H$_2$CH$_2$N). Anal. Calcd for C$_{32}$H$_{34}$N$_5$Br$_3$: C 52.77; H 4.71; N 9.62 %. Found: C 52.61; H 4.52; N 9.73 %.

Synthesis of 6 and 7: 4 or **5** (9 mmol), H$_2$O (100 mL) and Et$_3$N (1.8 g, 17 mmol) were added to a flask. The mixture was stirred at room temperature for 30 min. Then, NH$_4$PF$_6$ (5.7 g, 35 mmol) was added slowly to precipitate a white solid, which was filtered and washed with H$_2$O to afford product as a white solid.

6: 4.8 g (88 % yield). ^{1}H NMR (CD$_3$CN, 400 MHz): δ 8.80 (s, 2H, NC*H*N), 7.75−7.85 (m, 4H, bzim), 7.59−7.73 (m, 4H, bzim), 4.41 (t, *J* = 5.6 Hz, 4H, bzimC*H*$_2$CH$_2$N), 3.96 (s, 6H, bzimC*H*$_3$), 3.08 (br, 4H, bzimCH$_2$C*H*$_2$N), 1.63 (br, 1H, N*H*). ^{13}C NMR (CD$_3$CN, 100 MHz): δ 142.2 (N*C*N), 132.7 (bzim), 132.1 (bzim),

127.6 (bzim), 127.5 (bzim), 113.9 (bzim), 113.9 (bzim), 47.7 (bzimCH_2*C*H_2N), 47.6 (bzim*C*H_2CH_2N), 33.9 (bzim*C*H_3). Anal. Calcd for $C_{20}H_{25}N_5F_{12}P_2$: C 38.41; H 4.03; N 11.20 %. Found: C 38.22; H 4.12; N 11.35 %. ESI-MS: *m/z* 167.58 $[M-2PF_6]^{2+}$, 334.25 $[M-2PF_6-H]^+$, 480.17 $[M-PF_6]^+$.

7: 6.2 g (92 % yield). ^{1}H NMR (DMSO-d_6, 400 MHz): δ 9.80 (s, 2H, NC*H*N), 8.01 (d, *J* = 8 Hz, 2H, Ph), 7.92 (d, *J* = 8 Hz, 2H, Ph), 7.54−7.68 (m, 4H, bzim), 7.27−7.52 (m, 10H, Ph and bzim), 5.72 (s, 4H, PhCH_2), 4.54 (br, 4H, bzimC$H_2$$CH_2$N), 3.08 (br, 4H, bzim$CH_2CH_2$N), 2.39 (br, 1H, N*H*). ^{13}C NMR (DMSO-d_6, 100 MHz): δ 142.6 (N*C*N), 134.0, 131.4, 130.7, 128.9, 128.7, 128.1, 126.6, 126.5, 113.8, 113.7, 49.7 (Ph*C*H_2), 46.8 (bzimCH_2*C*H_2N), 46.4 (bzim*C*H_2CH_2N). Anal. Calcd for $C_{32}H_{33}N_5F_{12}P_2$: C 49.43; H 4.28; N 9.01 %. Found: C 49.27; H 4.15; N 8.87 %. ESI-MS: *m/z* 243.67 $[M-2PF_6]^{2+}$, 486.33 $[M-2PF_6-H]^+$, 632.25 $[M-PF_6]^+$.

Synthesis of 8 and 9. A mixture of **6** or **7** (0.24 mmol) and Ag_2O (111 mg, 0.48 mmol) in 5 mL of acetonitrile was stirred at room temperature for 24 hours. After that, the mixture was filtered. Vapor diffusion of ether to the filtrate to give colorless crystals.

8: 162 mg (95 % yield). ^{1}H NMR (DMSO-d_6, 400 MHz): δ 7.86−8.12 (m, 6H, bzim), 7.42−7.83 (m, 10H, bzim), 4.52−5.25 (br, 8H, bzimC$H_2$$CH_2$N), 4.16 (br, 8H, bzim$CH_2CH_2$N), 3.68 (br, 2H, N*H*), 2.92−3.38 (br, 12H, bzimCH_3). ^{13}C NMR (DMSO-d_6, 100 Hz): δ 186.4 (NCN), 183.7 (bzim), 134.5 (134.5) (bzim), 133.6 (bzim), 133.2 (bzim), 124.9 (bzim), 124.9 (bzim), 124.3 (bzim), 124.3 (bzim), 112.5 (bzim), 112.4 (bzim), 112.3 (bzim), 111.8 (bzim), 51.7 (*C*H_2), 51.4 (*C*H_2), 50.8 (*C*H_2),

48.8 (*C*H_2), 35.5 (*C*H_3), 35.0 (*C*H_3). Anal. Calcd for $C_{40}H_{46}Ag_3N_{10}F_{18}P_3$: C 33.71; H 3.25; N 9.83 %. Found: C 33.52; H 3.13; N 9.65 %. ESI-MS: *m/z* 440.33 $[M-Ag-3PF_6]^{2+}$.

9: 174 mg (84 % yield). Anal. Calcd for $C_{64}H_{62}Ag_3N_{10}F_{18}P_3$: C 44.44; H 3.61; N 8.10 %. Found: C 44.18; H 3.45; N 8.23 %. ESI-MS: 594.33 $[M-Ag-3PF_6]^{2+}$.

Synthesis of 10 and 11

Route 1: 5 mL of acetonitrile was added to a mixture of **6** or **7** (0.24 mmol) and Cu_2O (343 mg, 2.40 mmol). The mixture is heated to reflux for 48 hours under nitrogen and then cooled to room temperature. Under nitrogen, the mixture was filtered. Vapor diffusion of ether to the filtrate to give green crystals.

Route 2: 8 or **9** (0.10 mmol) and CuCl (30 mg, 0.30 mmol) were mixed in 5 mL of acetonitrile. The resulting mixture was stirred at room temperature for 24 hours. Then, under nitrogen, the mixture was filtered. Vapor diffusion of ether to the filtrate to yield the product as green crystals.

10: 112 mg (86 % yield) (route 1); 20 mg (38% yield) (route 2). ^{1}H NMR (DMSO-d_6, 400 MHz): δ 7.68−7.84 (m, 4H, bzim), 7.36−7.51 (m, 4H, bzim), 4.44 (br, 4H, bzimC*H*$_2$CH$_2$N), 4.17 (s, 6H, bzimC*H*$_3$), 4.06 (br, 1H, N*H*), 3.24 (br, 4H, bzimCH$_2$C*H*$_2$N). ^{13}C NMR (DMSO-d_6, 100 MHz): δ 188.8 (N*C*N), 134.3 (bzim), 133.2 (bzim), 123.3 (bzim), 123.2 (bzim), 111.4 (bzim), 110.9 (bzim), 49.3 (bzimCH$_2$*C*H$_2$N), 44.7 (bzim*C*H$_2$CH$_2$N), 35.0 (bzim*C*H$_3$). Anal. Calcd for $C_{20}H_{23}N_5CuF_6P$: C 44.33; H 4.28; N 12.92%. Found: C 44.18; H 4.36; N 12.77%. ESI-MS: *m/z* 396.33 $[M-PF_6]^+$.

11: 57 mg (34 % yield) (route 1); 15 mg (22% yield) (route 2). ^{1}H NMR (CD_3CN, 400 MHz): δ 7.58−7.64 (m, 4H, bzim), 7.35-7.42 (m, 4H, bzim), 7.14-7.32 (m, 10H, Ph). ^{13}C NMR (CD_3CN, 100 MHz): δ 190.0 (N*C*N), 137.1 (Ph), 136.8 (bzim), 133.3 (bzim), 129.3 (Ph), 128.5 (Ph), 127.5 (Ph), 124.2 (124.2) (bzim), 112.4 (bzim), 111.6 (bzim), 52.7 (Ph*C*H_2), 50.1 (bzimCH_2*C*H_2N), 46.1 (bzim*C*H_2CH_2N). Anal. Calcd for $C_{32}H_{31}N_5CuF_6P$: C 55.37; H 4.50; N 10.09 %. Found: C 55.18; H 4.67; N 10.15 %. ESI-MS: *m/z* 548.33 $[M-PF_6]^+$.

Synthesis of 12: A mixture of **8** (162 mg, 0.11 mmol) and CuCl (22 mg, 0.22 mmol) in 5 mL of acetonitrile was stirred at room temperature for 24 hours. Then, under nitrogen, the mixture was filtered. Vapor diffusion of ether to the filtrate to give **12** as light yellow crystals (27 mg, 18 % yield). ^{1}H NMR (DMSO-d_6, 400 MHz): δ 7.68−7.86 (m, 8H, bzim), 7.37−7.48 (m, 8H, bzim), 4.44 (br, 8H, bzimC*H*$_2$CH_2N), 4.15 (s, 12H, bzimCH_2C*H*$_2$N), 4.07 (br, 2H, N*H*), 3.24 (br, 8H, bzimC*H*$_3$), 2.06 (s, 6H, C*H*$_3$CN). ^{13}C NMR (DMSO-d_6, 100 MHz): δ 187.8 (N*C*N), 134.2 (bzim), 133.2 (bzim), 123.2 (bzim), 123.1 (bzim), 117.9 (CH$_3$*C*N), 111.3 (bzim), 110.8 (bzim), 49.1 (bzimCH$_2$*C*H$_2$N), 44.5 (bzim*C*H$_2$CH$_2$N), 35.0 (bzim*C*H$_3$), 1.0 (*C*H$_3$CN). Anal. Calcd for $C_{44}H_{52}N_{12}Cu_2AgF_{18}P_3$: C 37.25; H 3.69; N 11.85 %. Found: C 37.45; H 3.88; N 12.03%. ESI-MS: *m/z* 396.25 $[Cu(L^1)]^+$.

Conversion of 12 into 10: **12** (20 mg, 0.014 mmol), CuCl (7 mg, 0.07 mmol) and acetonitrile (2 mL) were added to a flask. The light yellow mixture was stirred at room temperature for 12 hours. Then, under nitrogen, the mixture was filtered and purified by vapor diffusion of ether to obtain green crystals. Examination by ^{1}H NMR

spectra, ESI-MS and X-ray diffraction analyses confirmed the formation of **10**.

X-ray Crystallography

X-ray diffraction data were collected on a Bruker APEX DUO diffractometer with a CCD area detector (Mo Kα radiation, λ = 0.71073 Å), which were integrated through the SAINT.[29] Absorption corrections were employed using the program SADABS.[30] The crystal structures were solved by the direct method using SHELXS-97[31] and subsequently completed by Fourier recycling using SHELXL 2014 program.[32] Non-hydrogen atoms were refined by anisotropic displacement parameters. Crystallographic data, data collection and refinement parameters for **8-12** are listed in Tables S1 and S2 in the SI.

DFT and TD-DFT Calculations

All the calculations were implemented in Gaussian 09 program package.[33] Firstly, the structures of the two mononuclear three-coordinate Cu(I)−NHC complexes **10** and **11** no considering the anion and solvent molecules as isolated molecules in the ground state (S_0) and lowest-energy triplet state (T_1) were optimized in the gas phase, respectively, by density functional theory (DFT) method[34] without symmetry constraint. The initial structures were extracted from the crystallographically determined geometries. The gradient corrected correlation functional form PBE1PBE[35] was used to describe the exchange and correlation interaction. To analyse the spectroscopic properties of

complexes **10** and **11**, 80 singlet and 6 triplet excited-states were calculated in CH_3CN to determine the vertical excitation energies by time-dependent density functional theory (TD-DFT),[36] based on the optimized ground state (S_0) and lowest-energy triplet state (T_1) structures, respectively. The solvent effects of CH_3CN were taken into account by performing the self-consistent reaction field (SCRF) calculations using the polarizable continuum model method (PCM).[37] In these calculations, the Stuttgart-Dresden (SDD) basis set and the effective core potentials (ECPs) was used to describe the Cu atom,[38] while other non-metal atoms of N, C and H were described by the all-electron basis set of 6-31G**. Visualization of the frontier molecular orbitals were performed by GaussView. Ros & Schuit method[39] (C-squared population analysis method, SCPA) was supported to analyze the partition orbital composition by using Multiwfn 3.3 program.[40]

Conflicts of interest

There are no conflicts to declare.

Acknowledgments

We are grateful for the financial support from the Natural Science Grant of China (No. 21471078 to X.-T.C) and the U.S. National Science Foundation (CHE-1633870 to Z.-L.X).

Notes and references

1. (a) N. Armaroli, G. Accorsi, F. Cardinali, A. Listorti, *Top. Curr. Chem.*, 2007, **280**, 69; (b) A. Barbieri, G. Accorsi, N. Armaroli, *Chem. Commun.*, 2008, **19**, 2185; (c) D. R. McMillin, K. M. McNett, *Chem. Rev.*, 1998, **98**, 1201; (d) R. Czerwieniec, M. J. Leitl, H. H. H. Homeier, H. Yersin, *Coord. Chem. Rev.*, 2016, **325**, 2; (e) E. Cariati, E. Lucenti, C. Botta, U. Giovanella, D. Marinotto, S. Righetto, *Coord. Chem. Rev.*, 2016, **306**, 566; (f) D. V. Scaltrito, D. W. Thompson, J. A. O'Callaghan, G. J. Meyer, *Coord. Chem. Rev.*, 2000, **208**, 243; (g) A. Lavie-Cambot, M. Cantuel, Y. Leydet, G. Jonusauskas, D. M. Bassani, N. D. McClenaghan, *Coord. Chem. Rev.*, 2008, **252**, 2572; (h) H. V. R. Dias, H. V. K. Diyabalanage, M. G. Eldabaja, O. Elbjeirami, M. A. Rawashdeh-Omary, M. A. Omary, *J. Am. Chem. Soc*., 2005, **127**, 7489; (i) M. A. Omary, M. A. Rawashdeh-Omary, M. W. A. Gonser, O. Elbjeirami, T. Grimes, T. R. Cundari, H. V. K. Diyabalanage, C. S. P. Gamage, H. V. R. Dias, *Inorg. Chem*., 2005, **44**, 8200.

2. (a) G. F. Manbeck, W. W. Brennessel, R. Eisenberg, *Inorg. Chem*., 2011, **50**, 3431; (b) C.-W. Hsu, C.-C. Lin, M.-W. Chung, Y. Chi, G.-H. Lee, P.-T. Chou, C.-H. Chang, P.-Y. Chen, *J. Am. Chem. Soc*., 2011, **133**, 12085; (c) D. G. Cuttell, S.-M. Kuang, P. E. Fanwick, D. R. McMillin, R. A. Walton, *J. Am. Chem. Soc*., 2002, **124**, 6; (d) M. G. Crestani, G. F. Manbeck, W. W. Brennessel, T. M. McCormick, R. Eisenberg, *Inorg. Chem.*, 2011, **50**, 7172; (e) S. Igawa, M. Hashimoto, I. Kawata, M. Yashima, M. Hoshino, M. Osawa, *J. Mater. Chem. C*, 2013, **1**, 542.

3. (a) L. X. Chen, G. Jennings, T. Liu, D. J. Gosztola, J. P. Hessler, D. V. Scaltrito, G. J. Meyer, *J. Am. Chem. Soc.*, 2002, **124**, 10861; (b) L. X. Chen, G. B. Shaw, I. Novozhilova, T. Liu, G. Jennings, K. Attenkofer, G. J. Meyer, P. Coppens, *J. Am. Chem. Soc.*, 2003, **125**, 7022; (c) Z. A. Siddique, Y. Yamamoto, T. Ohno, K. Nozaki, *Inorg. Chem.*, 2003, **42**, 6366.
4. (a) M. Hashimoto, S. Igawa, M. Yashima, I. Kawata, M. Hoshino, M. Osawa, *J. Am. Chem. Soc*., 2011, **133**, 10348; (b) M. Osawa, *Chem. Commun.*, 2014, **50**, 1801; (c) M. Osawa, M. Hoshino, M. Hashimoto, I. Kawata, S. Igawaa, M. Yashimaa, *Dalton Trans.*, 2015, **44**, 8369; (d) K. J. Lotitoz, J. C. Peters, *Chem. Commun.*, 2010, **46**, 3690; (e) D. Kakizoe, M. Nishikawa, Y. Fujii, T. Tsubomura, *Dalton Trans.*, 2017, **46**, 14804.
5. (a) S. B. Harkins, J. C. Peters, *J. Am. Chem. Soc.*, 2005, **127**, 2030; (b) J. C. Deaton, S. C. Switalski, D. Y. Kondakov, R. H. Young, T. D. Pawlik, D. J. Giesen, S. B. Harkins, A. J. M. Miller, S. F. Mickenberg, J. C. Peters, *J. Am. Chem. Soc.*, 2010, **132**, 9499; (c) T. Hofbeck, U. Monkowius, H. Yersin, *J. Am. Chem. Soc.*, 2015, **137**, 399.
6. (a) M. Wallesch, D. Volz, D. M. Zink, U. Schepers, M. Nieger, T. Baumann, S. Bräse, *Chem. Eur. J*., 2014, **20**, 6578; (b) P. C. Ford, E. Cariati, J. Bourassa, *Chem. Rev.*, 1999, **99**, 3625; (c) K. Tsuge, *Chem. Lett.*, 2013, **42**, 204; (d) P. D. Harvey, M. Knorr, *Macromol. Rapid Commun.*, 2010, **31**, 808; (e) X.-L. Chen, R. Yu, X.-Y. Wu, D. Liang, J.-H. Jia, C.-Z. Lu, *Chem. Commun.*, 2016, **52**, 6288.
7. (a) W. A. Herrmann, *Angew. Chem. Int. Ed.*, 2002, **41**, 1290; (b) S. Díez-González,

N. Marion, S. P. Nolan, *Chem. Rev*., 2009, **109**, 3612; (c) F. Lazreg, F. Nahra, C. S. J. Cazin, *Coord. Chem. Rev.*, 2015, **293–294**, 48–79.

8. (a) R. Visbal, M. C. Gimeno, *Chem. Soc. Rev.*, 2014, **43**, 3551; (b) Y. Unger, D. Meyer, O. Molt, C. Schildknecht, I. Muenster, G. Wagenblast, T. Strassner, *Angew. Chem. Int. Ed.*, 2010, **49**, 10214; (c) K.-Y. Lu, H.-H. Chou, C.-H. Hsieh, Y.-H. O. Yang, H.-R. Tsai, H.-Y. Tsai, L.-C. Hsu, C.-Y. Chen, I. C. Chen, C.-H. Cheng, *Adv. Mater*., 2011, **23**, 4933.
9. (a) A. S. Romanov, D. Di, L. Yang, J. Fernandez-Cestau, C. R. Becker, C. E. James, B. Zhu, M. Linnolahti, D. Credgington, M. Bochmann, *Chem. Commun.*, 2016, **52**, 6379; (b) S. Shi, L. R. Collins, M. F. Mahon, P. I. Djurovich, M. E. Thompson, M. K. Whittlesey, *Dalton Trans.*, 2017, **46**, 745; (c) M. Gernert, U. Meller, M. Haehnel, J. Pflaum, A. Steffen, *Chem. Eur. J.*, 2017, **23**, 2206; (d) A. S. Romanov, C. R. Becker, C. E. James, D. Di, D. Credgington, M. Linnolahti, M. Bochmann, *Chem. Eur. J.*, 2017, **23**, 4625; (e) R. Hamze, R. Jazzar, M. Soleilhavoup, P. I. Djurovich, G. Bertrand, M. E. Thompson, *Chem. Commun.*, 2017, **53**, 9008.
10. (a) V. A. Krylova, P. I. Djurovich, M. T. Whited, M. E. Thompson, *Chem. Commun.*, 2010, **46**, 6696; (b) V. A. Krylova, P. I. Djurovich, J. W. Aronson, R. Haiges, M. T. Whited, M. E. Thompson, *Organometallics*, 2012, **31**, 7983; (c) V. A. Krylova, P. I. Djurovich, B. L. Conley, R. Haiges, M. T. Whited, T. J. Williams, M. E. Thompson, *Chem. Commun*., 2014, **50**, 7176; (d) M. J. Leitl, V. A. Krylova, P. I. Djurovich, M. E. Thompson, H. Yersin, *J. Am. Chem. Soc*., 2014,

136, 16032; (e) R. Marion, F. Sguerra, F. Di Meo, E. Sauvageot, J.-F. Lohier, R. Daniellou, J.-L. Renaud, M. Linares, M. Hamel, S. Gaillard, *Inorg. Chem*., 2014, **53**, 9181; (f) M. Elie, F. Sguerra, F. Di Meo, M. D. Weber, R. Marion, A. Grimault, J.-F. Lohier, A. Stallivieri, A. Brosseau, R. B. Pansu, J.-L. Renaud, M. Linares, M. Hamel, R. D. Costa, S. Gaillard. *ACS Appl. Mater. Interfaces*, 2016, **8**, 14678; (g) B. Hupp, C. Schiller, C. Lenczyk, M. Stanoppi, K. Edkins, A. Lorbach, A. Steffen, *Inorg. Chem.*, 2017, **56**, 8996.

11. Z. Wang, C. Zheng, W. Wang, C. Xu, B. Ji, X. Zhang, *Inorg. Chem*., 2016, **55**, 2157.
12. J. A. G. Williams, *Top. Curr. Chem.*, 2007, **281**, 205.
13. V. W.-W. Yam, E. C.-C. Cheng, *Top. Curr. Chem.*, 2007, **281**, 269.
14. C.-M. Che, S.-W. Lai, *Coord. Chem. Rev.*, 2005, **249**, 1296.
15. (a) K. Matsumoto, N. Matsumoto, A. Ishii, T. Tsukuda, M. Hasegawa, T. Tsubomura, *Dalton Trans.*, 2009, 6795; (b) M. Nishikawa, T. Sano, M. Washimi, K. Takao, T. Tsubomura, *Dalton Trans.*, 2016, **45**, 12127; (c) R. Zhong, A. Pöthig, D. C. Mayer, C. Jandl, P. J. Altmann, W. A. Herrmann, F. E. Kühn, *Organometallics*, 2015, **34**, 2573; (d) J. Nitsch, F. Lacemon, A. Lorbach, A. Eichhorn, F. Cisnetti, A. Steffen, *Chem. Commun.*, 2016, **52**, 2932; (e) V. J. Catalano, L. B. Munro, C. E. Strasser, A. F. Samin, *Inorg. Chem.*, 2011, **50**, 8465.
16. (a) C. E. Strasser, V. J. Catalano, *Inorg. Chem.*, 2011, **50**, 11228; (b) C. E. Strasser, V. J. Catalano, *J. Am. Chem. Soc.*, 2010, **132**, 10009; (c) K. Chen, M. M. Nenzel, T. M. Brown, V. J. Catalano, *Inorg. Chem*., 2015, **54**, 6900; (d) V. J.

Catalano, A. L. Moore, J. Shearer, J. Kim, *Inorg. Chem.*, 2009, **48**, 11362.

17. (a) V. J. Catalano, M. A. Malwitz, A. O. Etogo, *Inorg. Chem.*, 2004, **43**, 5714; (b) V. J. Catalano, A. O. Etogo, *J. Organomet. Chem.*, 2005, **690**, 6041; (c) V. J. Catalano, A. O. Etogo, *Inorg. Chem.*, 2007, **46**, 5608; (d) T. P. Pell, D. J. D. Wilson, B. W. Skelton, J. L. Dutton, P. J. Barnard, *Inorg. Chem*., 2016, **55**, 6882; (e) P. Ai, M. Mauro, L. De Cola, A. A. Danopoulos, P. Braunstein, *Angew. Chem. Int. Ed.,* 2016, **55**, 3338; (f) P. Ai, M. Mauro, C. Gourlaouen, S. Carrara, L. De Cola, Y. Tobon, U. Giovanella, C. Botta, A. A. Danopoulos, P. Braunstein, *Inorg. Chem.*, 2016, **55**, 8527.
18. T. Simler, P. A. A. Braunstein, *Angew. Chem. Int. Ed.*, 2015, **54**, 13691.
19. N. N. Al-Mohammed, Y. Alias, Z. Abdullah, R. M. Shakir, E. M. Taha, A. A. Hamid, *Molecules*, 2013, **18**, 11978.
20. (a) H. M. J. Wang, I. J. B. Lin, *Organometallics*, 1998, **17**, 972; (b) J. C. Garrison, W. J. Youngs, *Chem. Rev.*, 2005, **105**, 3978.
21. A. Melaiye, Z. Sun, K. Hindi, A. Milsted, D. Ely, D. H. Reneker, C. A. Tessier, W. J. Youngs*, J. Am. Chem. Soc*., 2005, **127**, 2285.
22. (a) V. J. Catalano, M. A. Malwitz, *Inorg. Chem.*, 2003, **42**, 5483; (b) V. J. Catalano, A. L. Moore, *Inorg. Chem.*, 2005, **44**, 6558; (c) J. C. Garrison, C. A. Tessier, W. J. Youngs, *J. Organomet. Chem.*, 2005, **690**, 6008; (d) X. Zhang, S. Gu, Q. Xia, W. Chen. *J. Organomet. Chem.*, 2009, **694**, 2359; (e) Y. Zhou, X. Zhang, W. Chen, H. Qiu, *J. Organomet. Chem.*, 2008, **693**, 205; (f) F. Li, S. Bai, T. S. A. Hor, *Organometallics*, 2008, **27***,* 672.

23. H. Schmidbaur, A. Schier, *Angew. Chem. Int. Ed.*, 2015, **54**, 746.

24. (a) G. Laus, K. Wurst, H. Schottenberger, *Z. Kristallogr. New Cryst. Struct.*, 2012, **227**, 413; (b) P. L. Chiu, C. Y. Chen, C.-C. Lee, M.-H. Hsieh, C.-H. Chuang, H. M. Lee, *Inorg. Chem.*, 2006, **45**, 2520; (c) J. Ye, W. Chen, D. Wang, *Dalton Trans*., 2008, **30**, 4015.

25. R. E. Andrew, C. M. Storey, A. B. Chaplin, *Dalton Trans*., 2016, **45**, 8937.

26. S. Sculfort, P. Braunstein, *Chem. Soc. Rev.*, 2011, **40**, 2741.

27. (a) C. E. Strasser, V. J. Catalano, *Inorg. Chem*., 2011, **50**, 11228; (b) V. J. Catalano, M. A. Malwitz, A. O. Etogo, *Inorg. Chem*., 2004, **43**, 5714; (c) V. J. Catalano, A. L. Moore, *Inorg. Chem*., 2005, **44**, 6558; (d) B. Liu, W. Chen, S. Jin, *Organometallics*, 2007, **26***,* 3660; (e) J. C. Garrison, R. S. Simons, W. G. Kofron, C. A. Tessier, W. J. Youngs, *Chem. Commun*., 2001, 1780; (f) S. Díez-González, E. C. Escudero-Adán, J. Benet-Buchholz, E. D. Stevens, A. M. Z. Slawin, S. P. Nolan, *Dalton Trans.*, 2010, **39**, 7595; (g) X. Han, L.-L. Koh, Z.-P. Liu, Z. Weng, T. S. Andy Hor, *Organometallics*, 2010, **29**, 2403.

28. (a) A. Tsuboyama, K. Kuge, M. Furugori, S. Okada, M. Hoshino, K. Ueno, *Inorg. Chem*., 2007, **46**, 1992; (b) C. Zeng, N. Wang, T. Peng, S. Wang, *Inorg. Chem.*, 2017, **56**, 1616.

29. SMART & SAINT Software Reference Manuals, version 6.45; Bruker Analytical X-ray Systems, Inc.: Madison, WI, 2003.

30. G. M. Sheldrick, SADABS: Software for Empirical Absorption Correction, version 2.05; University of Göttingen: Göttingen, Germany, 2002.

31. G. M. Sheldrick, SHELXS-1997, Program for Crystal Structure Solution, University of Göttingen, Göttingen, Germany, 2008.

32. G. M. Sheldrick, SHELXL2014: Program for Crystal Structure Refinement; University of Göttingen: Göttingen, Germany, 2014.

33. M. J. Frisch, G. W. Trucks, H. B. Schlegel, G. E. Scuseria, M. A. Robb, J. R. Cheeseman, G. Scalmani, V. Barone, B. Mennucci, G. A. Petersson, H. Nakatsuji, M. Caricato, X. Li, H. P. Hratchian, A. F. Izmaylov, J. Bloino, G. Zheng, J. L. Sonnenberg, M. Hada, M. Ehara, K. Toyota, R. Fukuda, J. Hasegawa, M. Ishida, T. Nakajima, Y. Honda, O. Kitao, H. Nakai, T. Vreven, J. A. Montgomery, Jr., J. E. Peralta, F. Ogliaro, M. Bearpark, J. J. Heyd, E. Brothers, K. N. Kudin, V. N. Staroverov, T. Keith, R. Kobayashi, J. Normand, K. Raghavachari, A. Rendell, J. C. Burant, S. S. Iyengar, J. Tomasi, M. Cossi, N. Rega, J. M. Millam, M. Klene, J. E. Knox, J. B. Cross, V. Bakken, C. Adamo, J. Jaramillo, R. Gomperts, R. E. Stratmann, O. Yazyev, A. J. Austin, R. Cammi, C. Pomelli, J. W. Ochterski, R. L. Martin, K. Morokuma, V. G. Zakrzewski, G. A. Voth, P. Salvador, J. J. Dannenberg, S. Dapprich, A. D. Daniels, O. Farkas, J. B. Foresman, J. V. Ortiz, J. Cioslowski, D. J. Fox. Gaussian 09, revision D.01. Gaussian, Inc., Wallingford CT, 2013.

34. A. D. Becke, *J. Chem. Phys.*, 1993, **98**, 5648.

35. J. P. Perdew, K. Burke, M. Ernzerhof, *Phys. Rev. Lett.*, 1996, **77**, 3865.

36. (a) R. Bauernschmitt, R. Ahlrichs, *Chem. Phys. Lett.*, 1996, **256**, 454; (b) M. E. Casida, C. Jamorski, K. C. Casida, D. R. Salahub, *J. Chem. Phys.*, 1998, **108**, 4439; (c) R. E. Stratmann, G. E. Scuseria, M. J. Frisch, *J. Chem. Phys*., 1998, **109**, 8218.

37. (a) V. Barone, M. Cossi, J. Tomasi, *J. Chem. Phys.*, 1997, **107**, 3210; (b) M. Cossi, G. Scalmani, N. Rega, V. Barone, *J. Chem. Phys.*, 2002, **117**, 43.

38. D. Andrae, U. Häussermann, M. Dolg, H. Stoll, H. Preuss, *Theor. Chim. Acta.*, 1990, **77**, 123.

39. P. Ros, G. C. A. Schuit, *Theor. Chim. Acta (Berl.)*, 1996, **4***,* 1.

40. T. Lu, F. W. Chen, *J. Comput. Chem.*, 2012, **33**, 580.

Synthesis, structures and luminescent properties of amine-bis(N-heterocyclic carbene) copper(I) and silver(I) complexes

Taotao Lu, Jin-Yun Wang, Lin-Xi Shi, Zhong-Ning Chen, Xue-Tai Chen, Zi-Ling Xue

Mononuclear Ag(I), Cu(I) and heterometallic Cu(I)/Ag(I) complexes with the tridentate amine-bis(N-heterocyclic carbene) were prepared, among which Cu(I)- and Cu/Ag complexes show luminescent properties.